Mechanical and Fluid Flow Properties of Basaltic Andesite and Rhyolite Analogue Rocks

SJ Bauer, P. Barrow, A. Robbins, M. Hileman, Sandia National Laboratories

Mechanical and fluid flow property determinations of the analogue lithologies were completed to exemplify test methods, provide estimates of these material properties in lieu of testing of samples gathered in situ, and to provide a data set for later comparison with data collected on in situ samples. Testing was completed by Sandia on andesite and rhyolite. The Limerick Greenstone and the Rochester Rhyolite are both part of the Lower Triassic Koipato Group. The Limerick "consists of altered porphyritic andesite flows and flow breccia and subordinate tuff and volcaniclastic rocks." The Rochester Rhyolite is described as consisting of "altered (albitized) felsite (probably ash-flow tuff) and beds and lenses of generally coarse-grained tuffaceous sedimentary rocks." The suite of measurements completed in varying numbers includes indirect tension, p- and s- wave velocity, density, unconfined compressive strength, confined compression, permeability during deformation, and natural tracer release during deformation.

Specimen Preparation and Experimental Methods

Specimen Preparation

Test specimens are right circular cylinders and were prepared from basaltic andesite and rhyolite, blocks collected from the FORGE field site vicinity and are judged representative lithologic equivalents.

Standard Practices for Preparing Rock Core as Cylindrical Test Specimens and Verifying Conformance to Dimensional and Shape Tolerances, ASTM D4543 – 08, is used to guide all specimen preparation. Specimen length, diameter, and aspect ratio depended on the test type. Beginning with each block, flats were cut on each block to provide a stable base to rest upon, and an opposing flat was cut to ease core barrel entry. Cores are taken with a water coolant diamond impregnated coring system and are either ~2.5 cm or ~3.75 cm outer diameter; the OD for all cores are ground to round using a wet lathe grinding system. Cores are cut to the approximate test length (test dependent) and compressive strength specimens are end ground parallel to each other and perpendicular to the core axis as described below. Samples are then dried for 24 hours in a 50C oven.

Calibration and data quality

Annual calibration of the measurement systems of force, length and mass are traceable to the U.S. National Institute of Standards and Technology. This includes loads cell used to measure compressive and tensile strength, displacement transducers used to measure displacement during strength testing, and scales for mass determinations. Based on the high standards of equipment calibration our lab is subjected to, and the ASTM standard testing techniques used, we consider the data presented to be high quality. The variations in material properties are then due to natural

heterogeneity of the rocks due to original conditions, and/or potential changes due to weathering from near surface exposure conditions.

Bulk Density Determination

The bulk density of each test specimen was determined by
dividing the mass by the volume where volume is calculated using dimensional measurements for the right-circular-cylindrical geometry.

Compressional and Shear Wave Velocity Measurements

Ultrasonic compressional and shear wave velocity measurements, Vp and Vs, were performed on each of the larger Brazil test specimens across specimen diameters, along long cores prior to cutting for UCS and triaxial testing, and some of the finished specimens along the long axis under ambient conditions prior to testing. These data are used to estimate the dynamic elastic properties.

The dynamic elastic Young's modulus, E_{dyn}, was determined directly from:

$$E_{dyn} = \rho V_s [(3V_p - 4V_s) / (V_p - V_s)]$$

Where ρ is the specimen density and Vp and Vs are the compressional and shear wave velocities, respectively.

Values of dynamic elastic Poisson's ratio, dynamic, were calculated from:

$$v_{dyn} = V_p^2 - V_s^2 / 2 (V_p^2 - V_s^2)$$

Tensile Strength

To determine the tensile strength, we used *ASTM D 3967-08, Standard Test Method for Splitting Tensile Strength of Intact Rock Core Specimens*. The tensile strength may be obtained by the direct uniaxial tensile strength, but this test is difficult and expensive for routine application. The splitting tensile test offers a desirable alternative. Engineers in rock mechanics design deal with complicated stress fields that include various combinations of compressive and tensile stress fields. One could argue that the tensile strength should be obtained with the presence of compressive and tensile stress conditions; the splitting tensile strength test, employed herein, is a simple test in which such stress fields occur.

In this test, typically a rock disk length/diameter = 0.5 is diametrically loaded between rigid platens (with bearing strips), until failure.

The splitting tensile strength is calculated as follows:

$\sigma_t = 2P/\pi LD$

where:

σ_t = Splitting tensile strength
P = Maximum applied load
L = Thickness of the specimen
D = Diameter of the specimen

Compressive Strength Testing

Standard Test Methods for Compressive Strength and Elastic Moduli of Intact Rock Core Specimens under Varying States of Stress and Temperatures, ASTM D7012 was used as a guide for all compressive strength testing, with specifics of tests noted when appropriate. In this test, typically a rock cylinder, length/diameter = 2 is axially loaded between rigid platens until failure. In the unconfined compressive strength test, (UCS) the confining or lateral pressure is ambient. For all UCS tests, displacement transducers are used to record axial and later displacement from which axial and lateral strains are determined and for triaxial tests, strain gages are bonded to the sample to recorded axial and lateral strains directly (Figure 1).

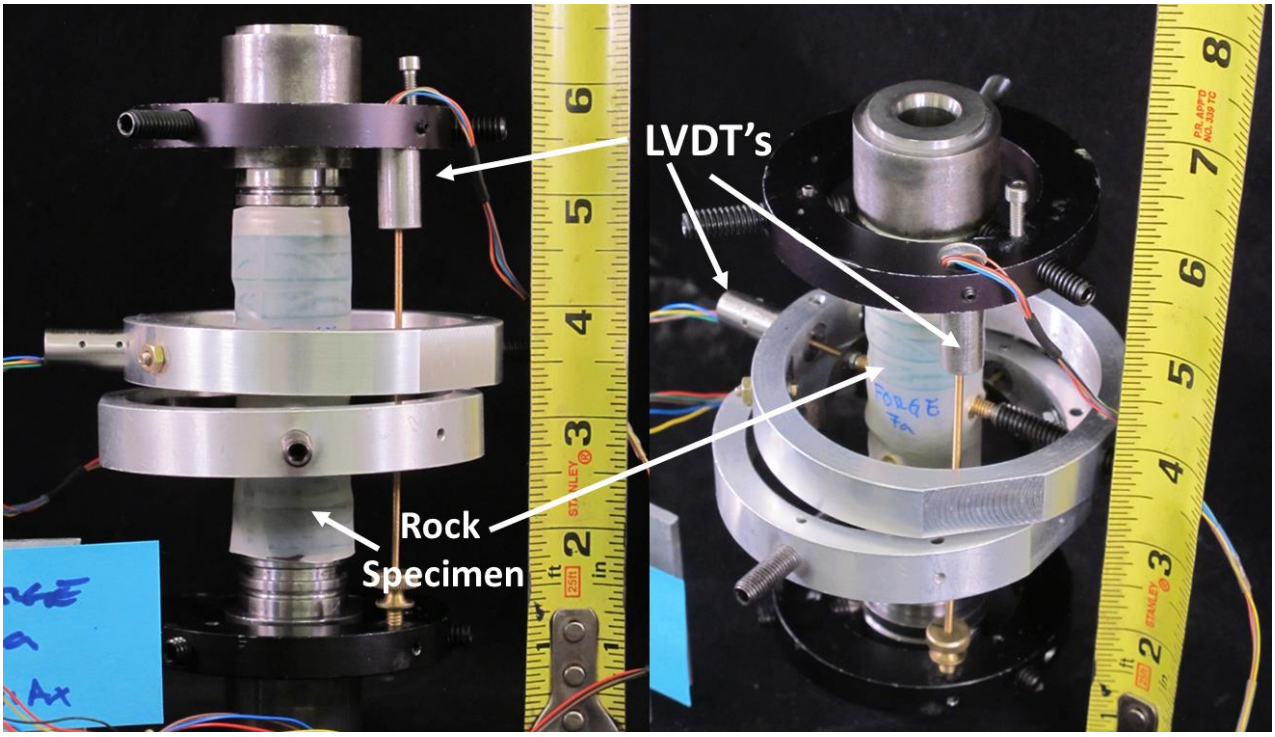

Figure 1. Instrumented specimen for UCS testing.

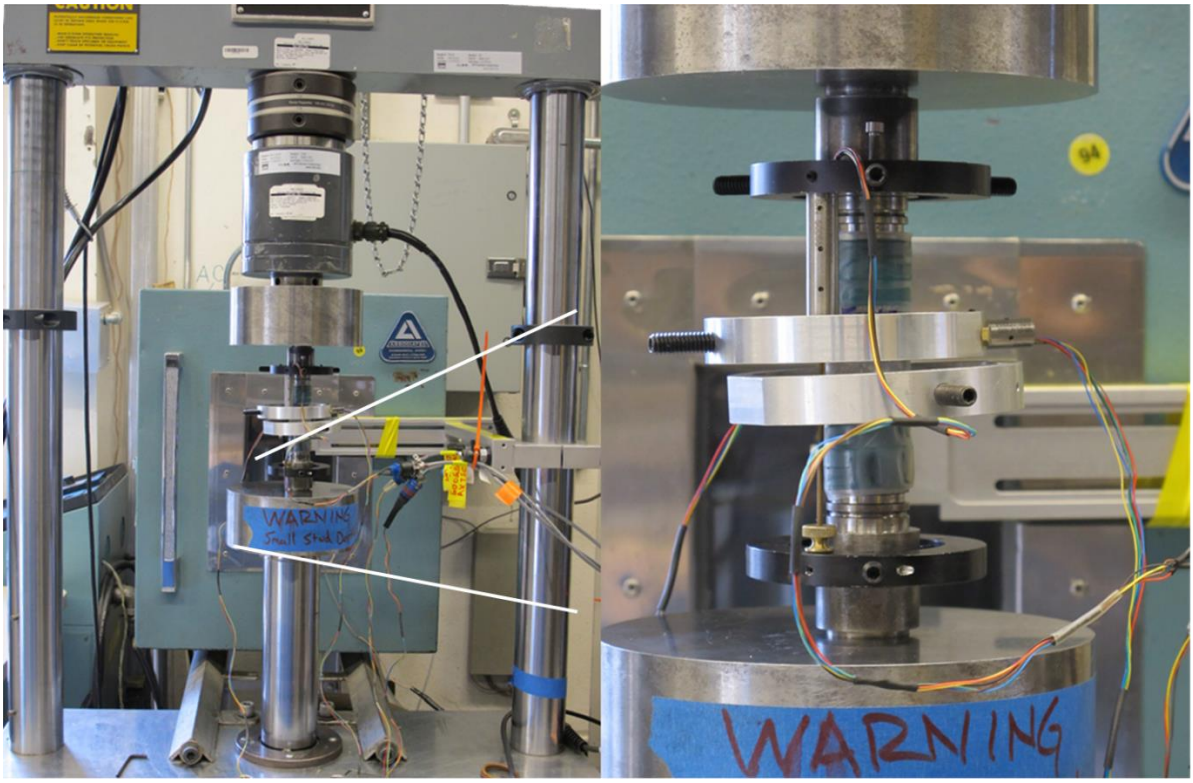

UCS Load frame Positioned Instrumented Specimen

Figure 2. UCS test frame and positioned instrumented specimen

Specimens were subjected to quasi-static compression loading at an axial strain rate of ~1e-^{05}/sec under ambient pressure and temperature conditions. Loading continued until the peak axial stress (i.e., the unconfined compressive strength) was determined. All specimens were loaded to failure. During loading, unload/reload cycles were performed at various axial stress levels to acquire data to estimate the quasi-static compressive elastic properties – Young's modulus, E, and Poisson's ratio, ν.

In a pressurized strength test, strain gaged jacketed samples are subjected to a hydrostatic confining pressure. During the pressurization, the confining pressure is increased and then decreased; these load- unload loops are used to calculate bulk modulus as a function of mean stress. One test of this type has been completed on the basaltic andesite, and in it permeability is determined at specific pressure and stress levels, as well as determination of the rock's strength at pressure.

Natural tracer release during deformation

In this type of experiment, a standard triaxial test is performed, excepting the pore system of a rock is accessed by a vacuum. During deformation, as the rock fractures, noble gases, if present

will be released from intracrystalline sites. Their release and real-time detection of noble gases has been shown to signal rock deformation (Bauer at al 2016).

Experimental Results

P- and S- wave velocities and dynamic elastic properties for the rhyolite and basaltic andesite are presented in Table 1 and Figures 1 and 2; dynamic elastic properties are presented in Figures 3 and 4. Velocities are presented versus density to demonstrate the direct relationship between velocity and density. The density of the basaltic andesite is consistently greater than that of the rhyolite. For the rhyolite, p- and s-wave velocity increase with increasing density, whereas for the basaltic andesite, p-wave velocity increases only slightly with density, and s-wave velocity remains about the same. For both rocks, the dynamic Young's modulus tend to increase with increasing density, whereas there is no clear trend in dynamic Poisson's ratio for the rhyolite, and an increasing trend for the basaltic rhyolite.

Table 1. Density, p- and s- wave velocity, dynamic elastic properties

Rock Type	*Density (g/cc)*	*P-wave (m/s)*	*S-wave (m/s)*	*E dynamic (GPa)*	*v dynamic*
Rhyolite	2.613	4892	2942	55.02	0.22
Rhyolite	2.613	5294	3172	64.15	0.22
Rhyolite	2.613	4935	2990	56.53	0.21
Rhyolite	2.585	4889	2673	47.53	0.29
Rhyolite	2.601	4965	2414	40.77	0.35
Rhyolite	2.622	4765	2851	52.06	0.22
Rhyolite	2.558	4572	2454	39.99	0.30
Rhyolite	2.617	5081	3692	67.10	-0.06
Rhyolite	2.622	5151	3177	63.13	0.19
Rhyolite	2.550	3643	1743	20.95	0.35
Rhyolite	2.592	4551	1979	28.08	0.38
Rhyolite	2.577	4346	1844	24.37	0.39
Rhyolite	2.604	4286	2273	35.08	0.30
Basaltic Andesite	2.742	5300	3013	62.80	0.26
Basaltic Andesite	2.716	5083	2604	48.70	0.32
Basaltic Andesite	2.701	5034	3019	60.02	0.22
Basaltic Andesite	2.664	4861	3103	59.31	0.16
Basaltic Andesite	2.675	4946	2908	55.92	0.24
Basaltic Andesite	2.693	4960	2796	53.34	0.27

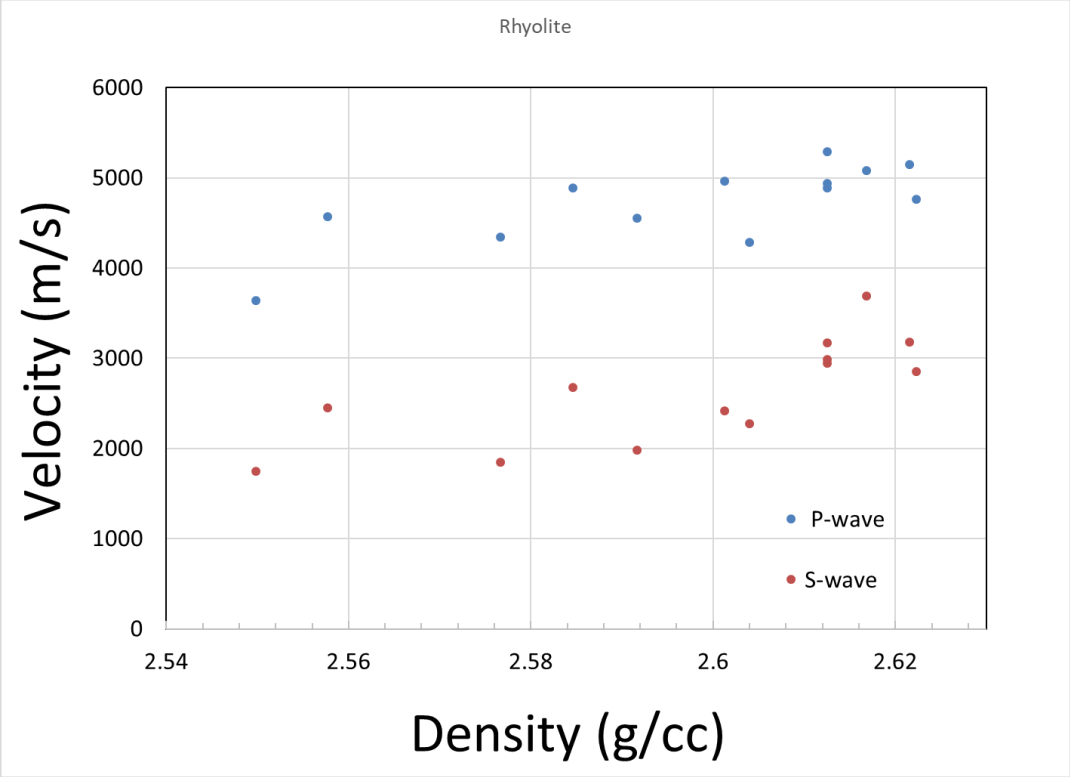

Figure 1. Rhyolite velocities versus density

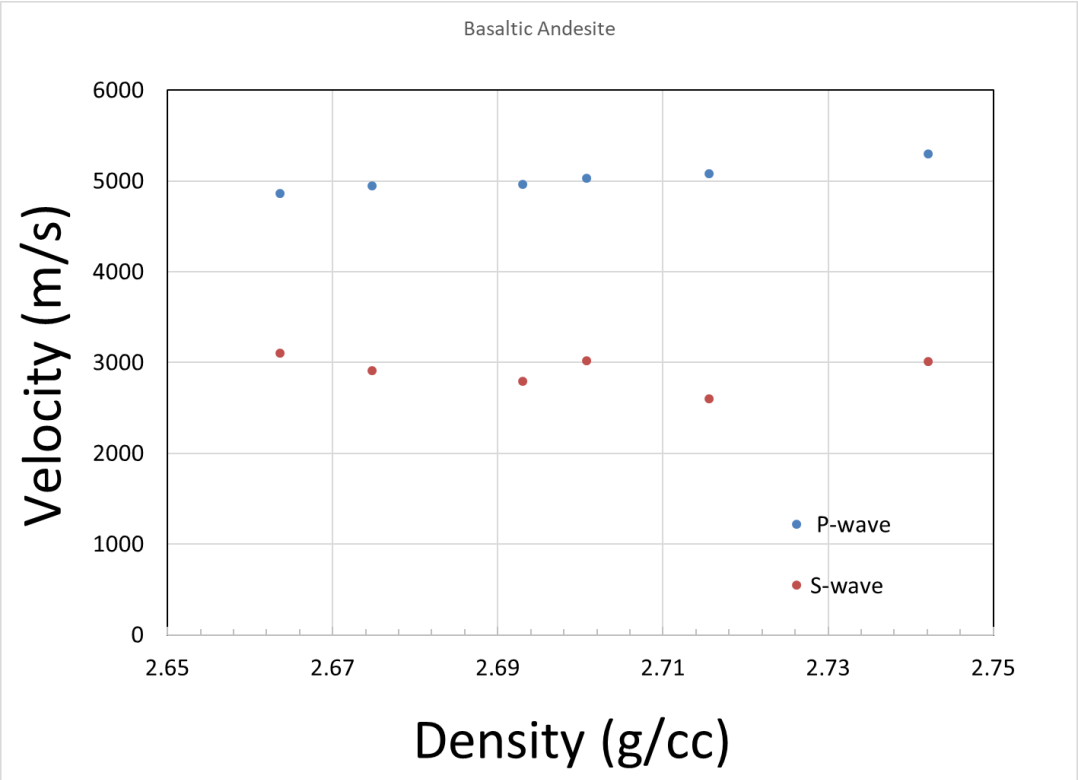

Figure 2. Basaltic andesite velocities versus density

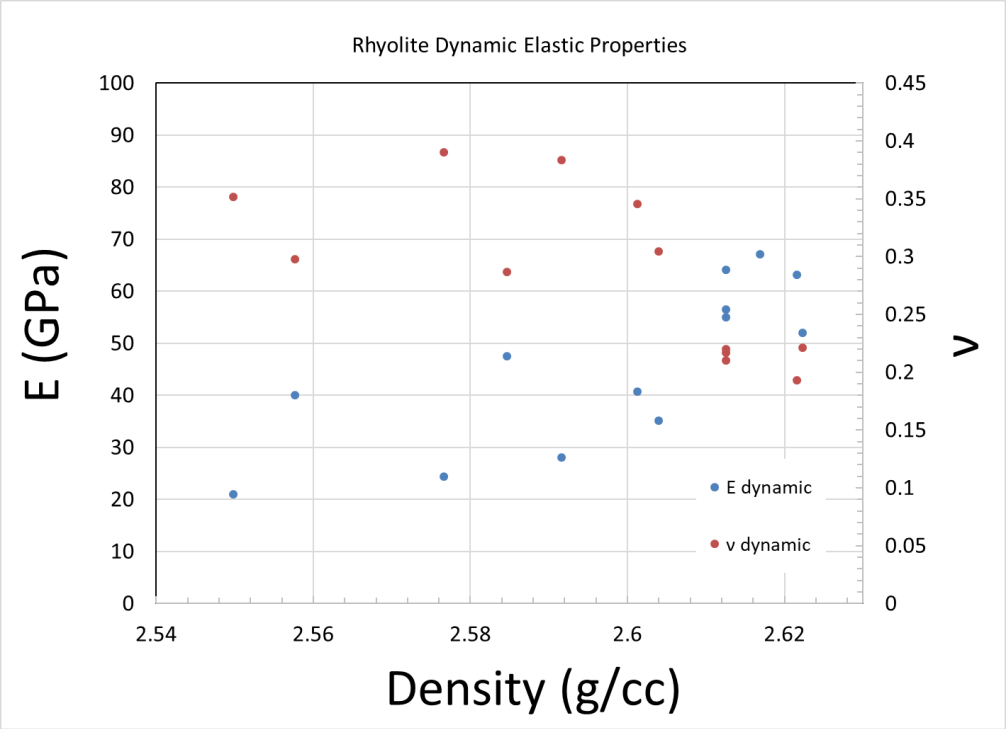

Figure 3. Rhyolite dynamic elastic properties versus density

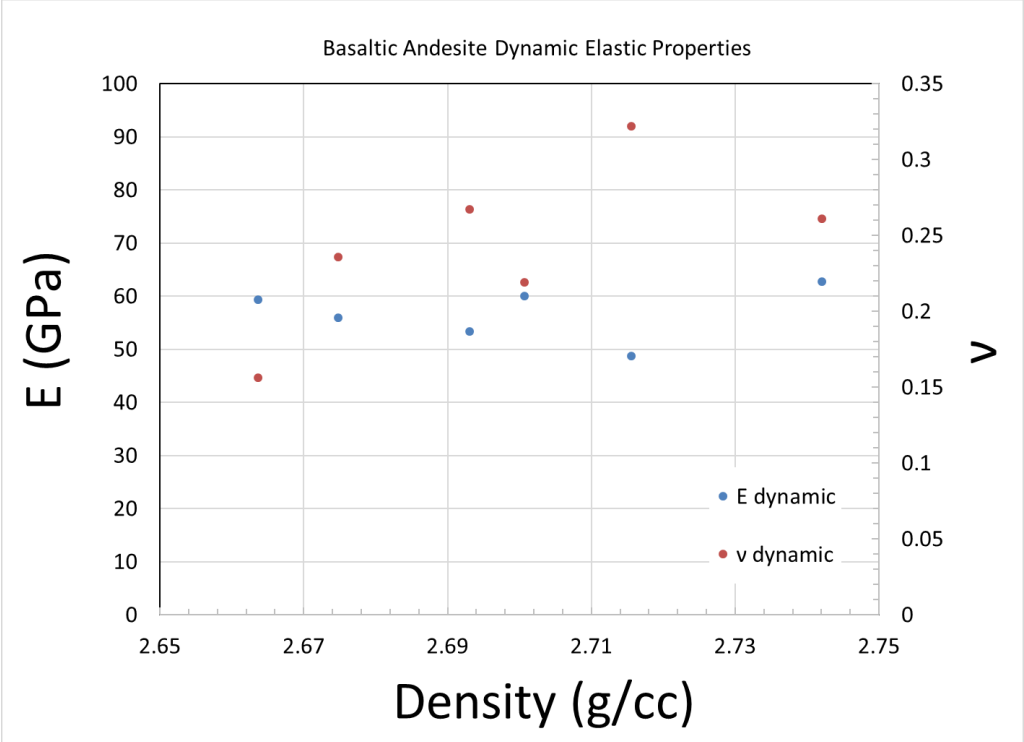

Figure 4. Basaltic andesite dynamic elastic properties versus density

Tensile strength of the rhyolite and basaltic andesite are presented in Table 2 and figures 5 and 6. The strength is plotted versus density and shows no apparent correlation. There are two strength groupings for each rock, for the rhyolite: 3 to 5 MPa, and ~8 MPa; for the basaltic andesite: 4 to 6 MPa, and 8-9 MPa. The lower strength band for each rock probably reflects the effect of fractures in the rocks, and the upper band may represent unfractured sampling.

Table 2. Tensile strength of basaltic andesite and rhyolite.

Rhyolite Specimen #	Tensile strength MPa
5a Brazil 1 (lat)	3.6
5a Brazil 2 (lat)	2.9
6a Brazil 1 (lat)	4.2
6a Brazil 2 (lat)	4.0
8a Brazil 1 (lat)	4.7
8b Brazil 1 (lat)	4.9
8b Brazil 2 (lat)	2.9
8b Brazil 3 (lat)	3.9
5b Brazil 1	8.5
5b Brazil 2	4.9
5b Brazil 3	5.2
5c Brazil 1	8.0
5c Brazil 2	8.3
Basaltic Andesite	
7a Brazil 1	7.9
7a Brazil 2	4.2
7a Brazil 3	3.9
3b Brazil 1	6.1
3b Brazil 2	5.5
3b Brazil 3	7.9
3c Brazil 1	9
3c Brazil 2	8.9
3c Brazil 3	3.8
7f Brazil 1	4.7

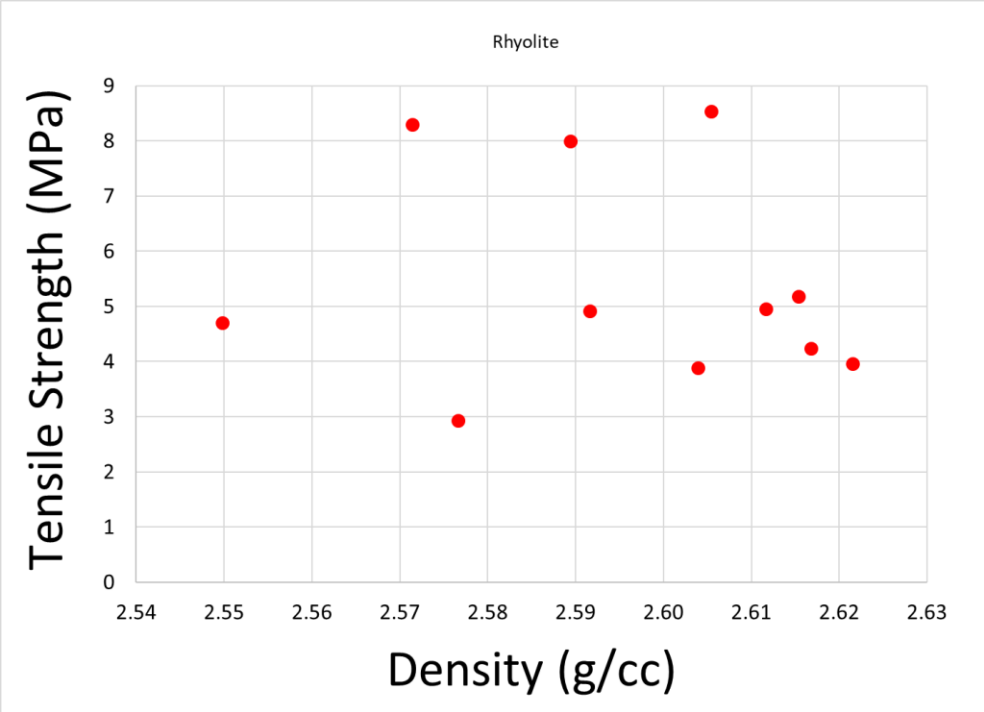

Figure 5. Rhyolite tensile strength versus density

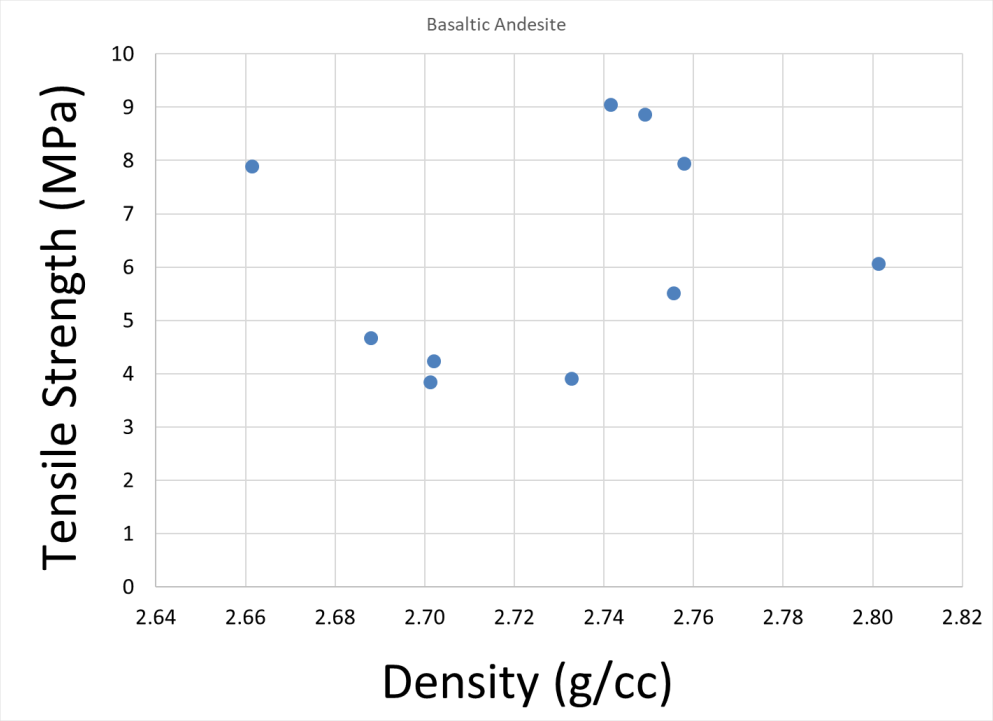

Figure 6. Basaltic andesite tensile strength versus density

Due to difficulty in coring, 5 specimens of the basaltic andesite were tested for UCS, and a single specimen of the rhyolite. Results of this effort are given in Table 2 and Figure 7. The strength of the basaltic andesite ranges from 86 to 203 MPa, with consistent strain to failure of less than 0.005. The single test of the rhyolite gave a UCS of 124 MPa and strain to failure of .0045. Static elastic property determinations as a function of increasing mean stress are presented in Table 3, 4 and Figure 8. These measurements are made on specimens tested at elevated pressure (the two triaxial experiments). The limited testing indicates a mild pressure dependence of Young's modulus with increasing mean stress, perhaps more pronounced for the basaltic andesite. This is sensible as microfractures should close with increasing stress (to a point).

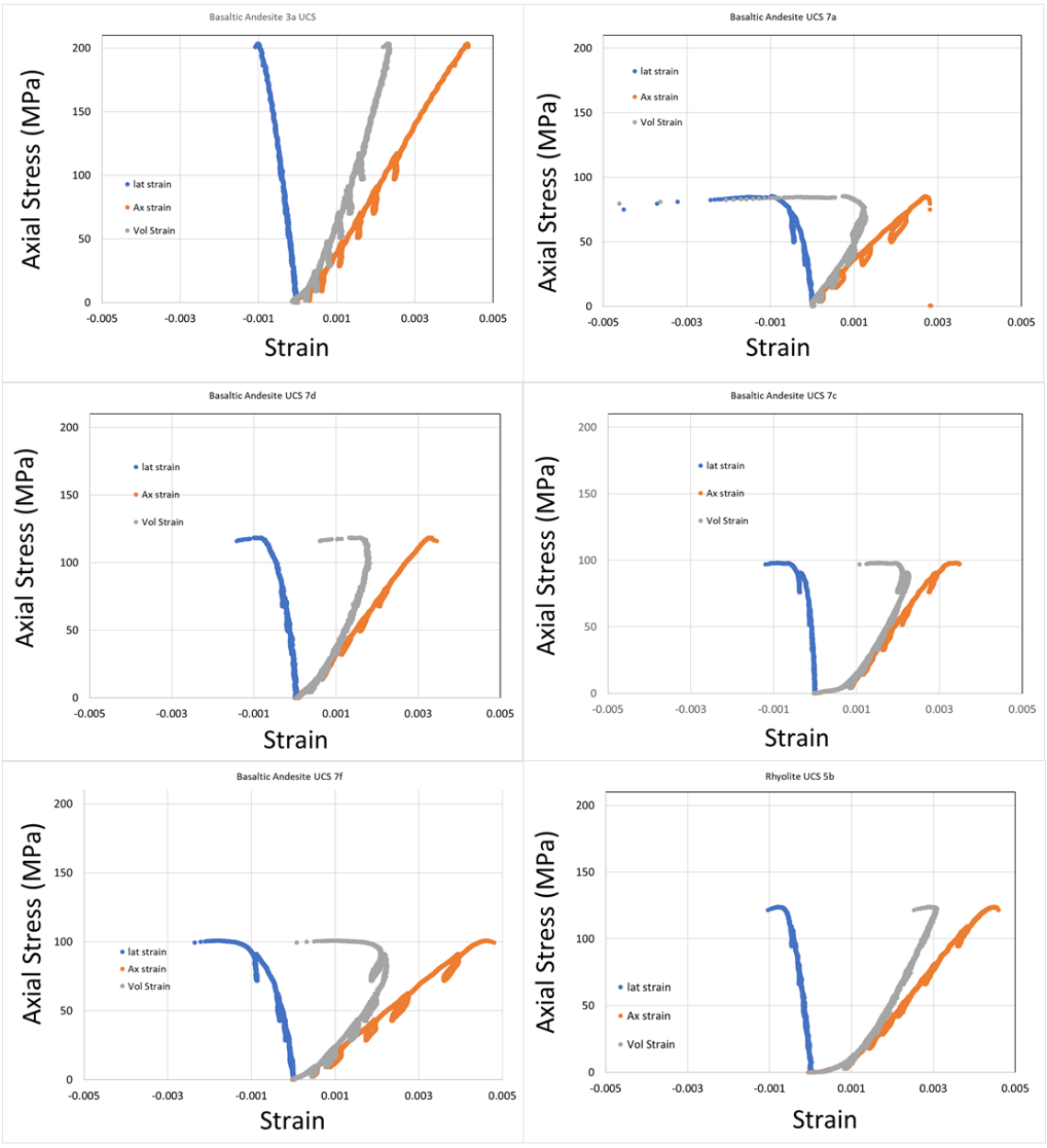

Figure 7. Unconfined Compressive strength

Table 2. Unconfined compressive strength and static elastic properties of rhyolite and basaltic andesite

Lithology	Specimen ID	UCS (MPa)	Axial Strain at Failure
Basaltic Andesite	3a	203	0.0044
Basaltic Andesite	7a	86	0.0028
Basaltic Andesite	7c	98	0.0033
Basaltic Andesite	7d	118	0.0033
Basaltic Andesite	7f	101	0.0047
Rhyolite	5b	124	0.0045

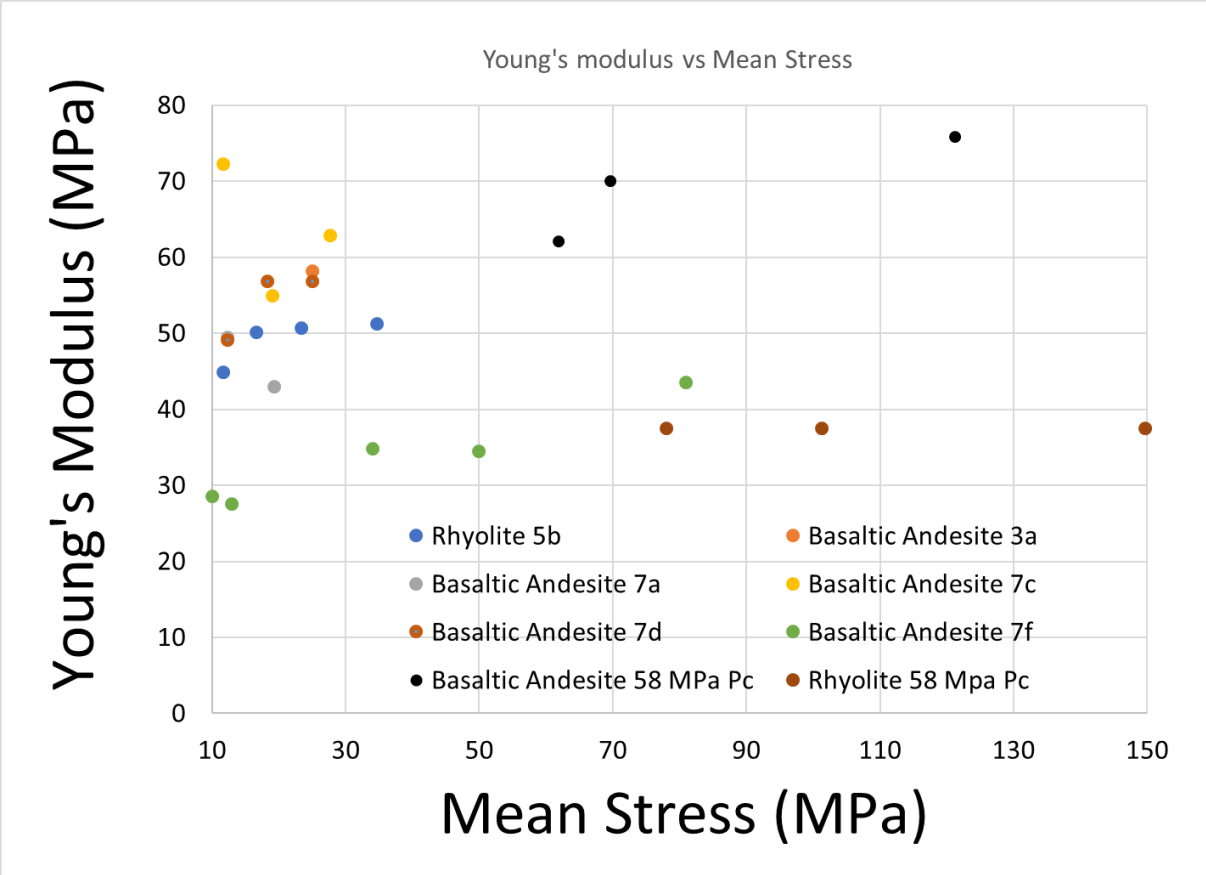

Figure 8. Young's Modulus versus Mean Stress for rhyolite and basaltic andesite

Table 3. Static elastic properties from UCS tests for rhyolite and basaltic andesite.

Rhyolite 5b	Mean Stress (MPa)	Young's Modulus (MPa)	Poisson's Ratio
	2.7	36.5	
	7.3	46.3	
	11.7	44.9	0.14
	16.7	50.1	0.1
	23.3	50.7	0.11
	34.7	51.2	0.11
Basaltic Andesite 3a	25.0	58.2	
Basaltic Andesite 7a	1.7	32	
	6.0	36.8	
	12.3	49.4	0.1
	19.3	43	0.17
Basaltic Andesite 7c	1.8	34.4	
	6.7	51.1	
	11.7	72.3	
	19.0	54.9	0.1
	27.7	62.9	0.1
Basaltic Andesite 7d	2.7	39.3	0.14
	6.7	46.4	0.13
	12.3	49.1	0.21
	18.3	56.8	0.11
	25.0	56.8	0.16
Basaltic Andesite 7f	3.3	28.5	
	4.3	27.6	0.14
	11.3	34.8	0.12
	16.7	34.5	0.13
	27.0	43.5	0.15

Table 4. Static Young's modulus and bulk modulus of rhyolite and basaltic andesite

	Mean Stress $(\sigma_1+ \sigma_2 +\sigma_3)/3$ (MPa)	Bulk Modulus (GPa)	Young's Modulus (MPa)
Rhyolite	17	24.5	
	30	25.6	
	45	27.3	
Rhyolite	78.0		37.5
	101		37.5
	150		37.5
Basaltic Andesite	62		62
	70		70
	121		76

Triaxial Experiments Results

Two triaxial experiments were completed and reported on. In the first test, gas flow through a specimen is continuously monitored during pressurization and application of deviatoric loading. In the second test, the specimen is treated as a closed system, and a vacuum is continuously applied to the specimen during pressurization and axial loading; the helium gas released and sensed may then be used to "signal" deformation.

In the first test, a specimen of basaltic andesite is strain gaged and jacketed and subjected to 48 MPa confining pressure. The pressure was chosen to be considerate of the subsurface target zone for the FORGE site. In the first test, helium is used as a permeant to flow through the specimen continuously during testing. The helium molecule is small and moves quickly though permeable systems, even low permeable ones. We used an upstream pressure ranging from 20 psi to 40 psi, depending on the flow sensing device. We used an Alicat 0-0.5 scc/min flow meter for high flow rate conditions, and an Oerlicon helium leak detector for low flow rate conditions. In this test we initially pressurized the specimen to 6.9 MPa confining pressure and measured flow rate and determined permeability during pressurization up to the 48 MPa test pressure, this flow information is not presented in this report; the raw data is in the data file. The flow-through testing methods may be found in Lee and Bauer (2015) and Bauer et al (2017).

The strength of the basaltic andesite at 48 MPa confining pressure is 300 MPa at ~0.02 axial strain. The "failure" is characterized by decrease in load carrying capacity and gentle decrease in load with increasing axial strain (Figure 9). The deformation was pushed ~ 0.0125 strain beyond failure to shed light on relating shear displacement to flow (and permeability). The deformed specimen shows a broad shear zone, as well as many pre-existing fractures in the sample. Perhaps some family of these fractures was activated in the deformation; this remains to be studied.

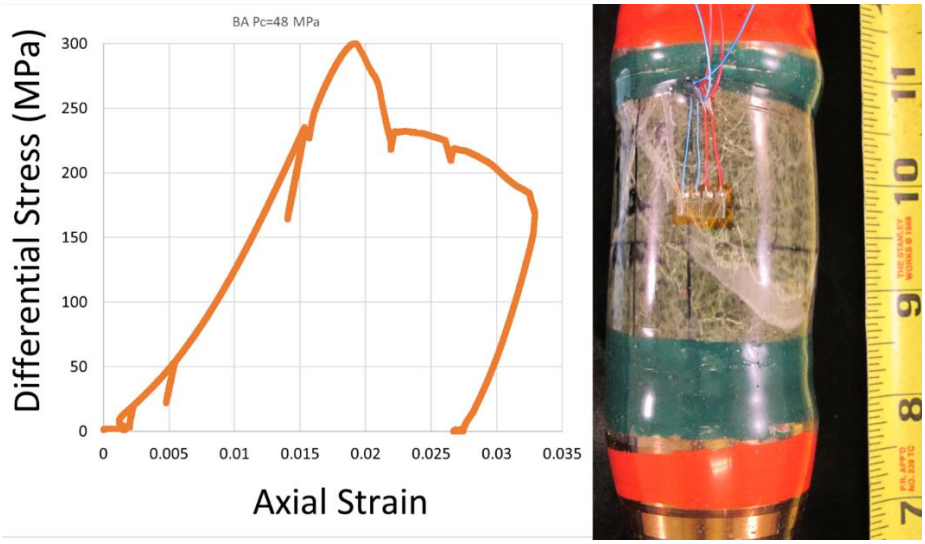

Figure 9. Axial stress versus axial strain for andesitic basalt specimen, and deformed specimen.

Figure 10 displays a time segment (25,000 sec) of the experiment, wherein axial strain and helium flow rate are plotted versus time. Flow rate is proportional to permeability (not determined herein due to time constraints) in this very small strain experiment, that is, changes in flow rate should be construed as permeability changes.

At point "1" below, loading was reinitiated after a hold period (note to the reader: one can relate the stress strain response in Figure 9 to the strains in Figure 10 by comparing strains). As axial strain is increased, flow rate decreases, suggesting that permeability is decreasing. In the "1" to "1'" straining period, the specimen yields and softens a bit. During this strain, the flow rate increased dramatically, and understandably because new fractures are formed. In the next time periods, flow rate decreases only slightly as minor amounts of strain accumulates. At arrowed time instances, strain, presumably slip along fracture surfaces, is accompanied by increases in flow rate. At point "2", the specimen is unloaded, flow rate increases slightly again, this probably is caused by opening of fractures during the unloading. However, this increase in flow does not continue to increase, indicating that most of the deformation imposed was permeant.

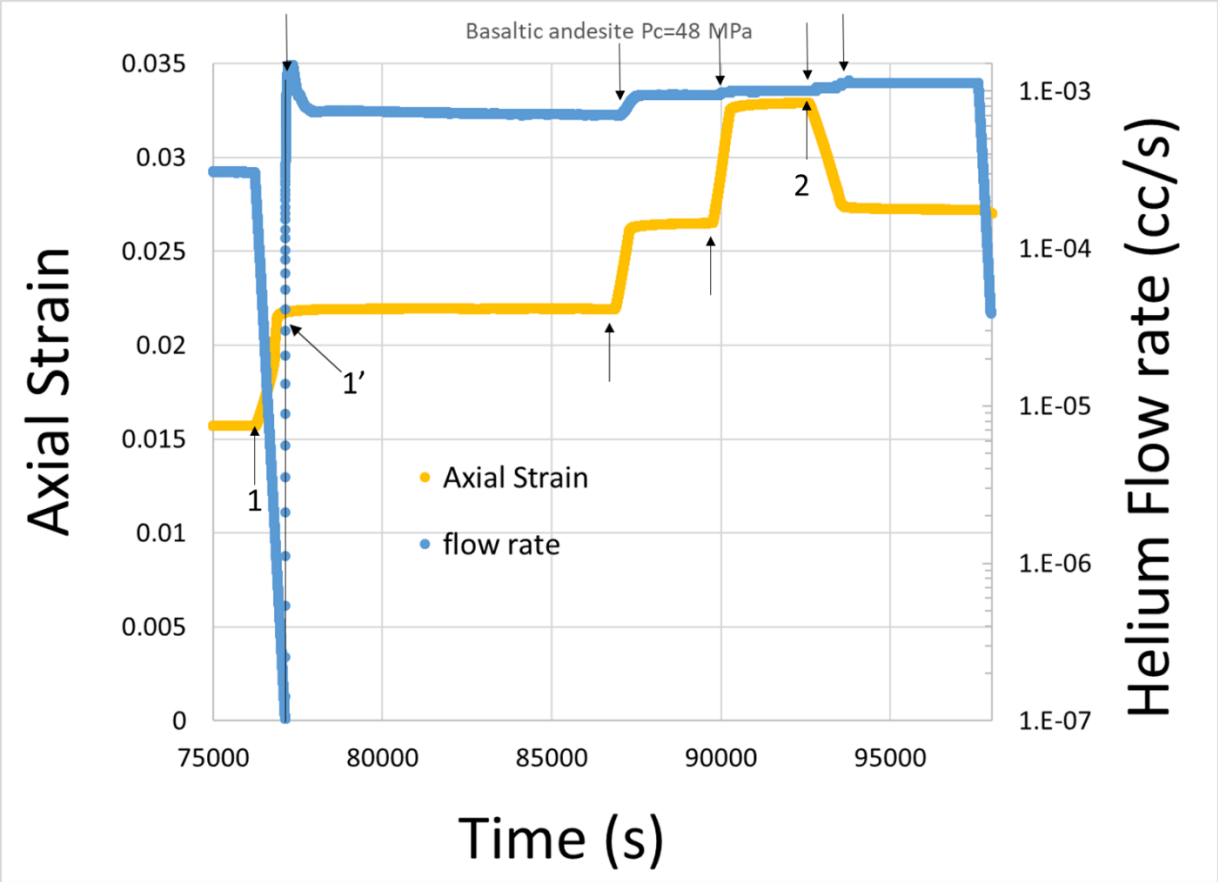

Figure 10. Axial strain and helium flow versus time.

Noble Gas Release Experiment

A single specimen of rhyolite was deformed in triaxial compression (48 MPa confining pressure) to failure at an axial strain rate of 10 e^{-5} at while monitoring real-time noble gas (^{4}He) release. The rhyolite specimen used is ~ 3.8 cm in diameter, and ~7.2 cm in length, a bit short of the standard length. The specimen also contained numerous cracks and microcracks. The stress strain response shown below displays a strength of on the order ~380 MPa, with initial yield/fracture at ~360 MPa (Figure 11). Coincident with yield/fracture is a dramatic increase in the number of acoustic emissions, an established signal of microfracturing. During the strain period following yield/fracture, acoustic emissions continue to accumulate.

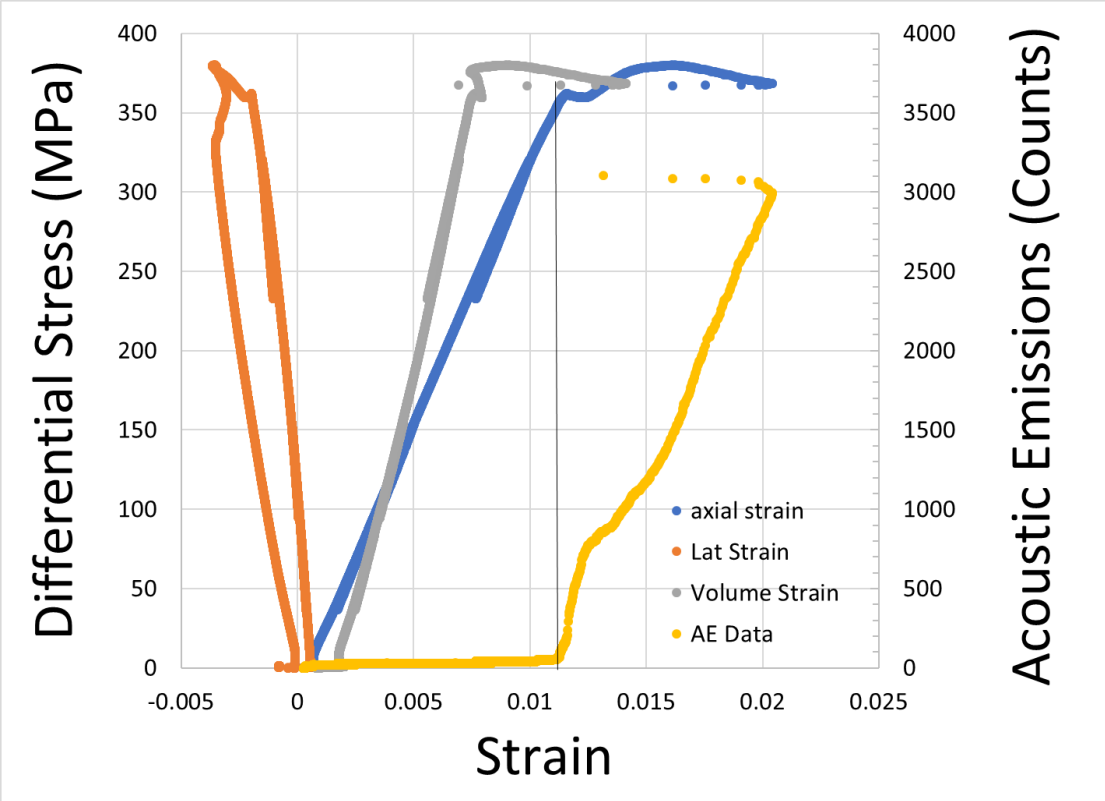

Figure 11. Stress strain behavior and acoustic emissions of rhyolite deformed at 48 MPa confining pressure.

During the experiment, helium flow from the specimen was recorded (Figure 12). Axial strain versus time shows the saw-toothed strain versus time imposed by the unload reload loops (from which we determine the deformation modulus). As the specimen accumulates strain beyond about 0.01, the flow rate of helium increases dramatically, consistent with the yield/fracture described above. During continued deformation, along a system of fractures, helium flow rate continues to increase, indicating additional fracturing, exposing fresh fracture sites for gas to be released.

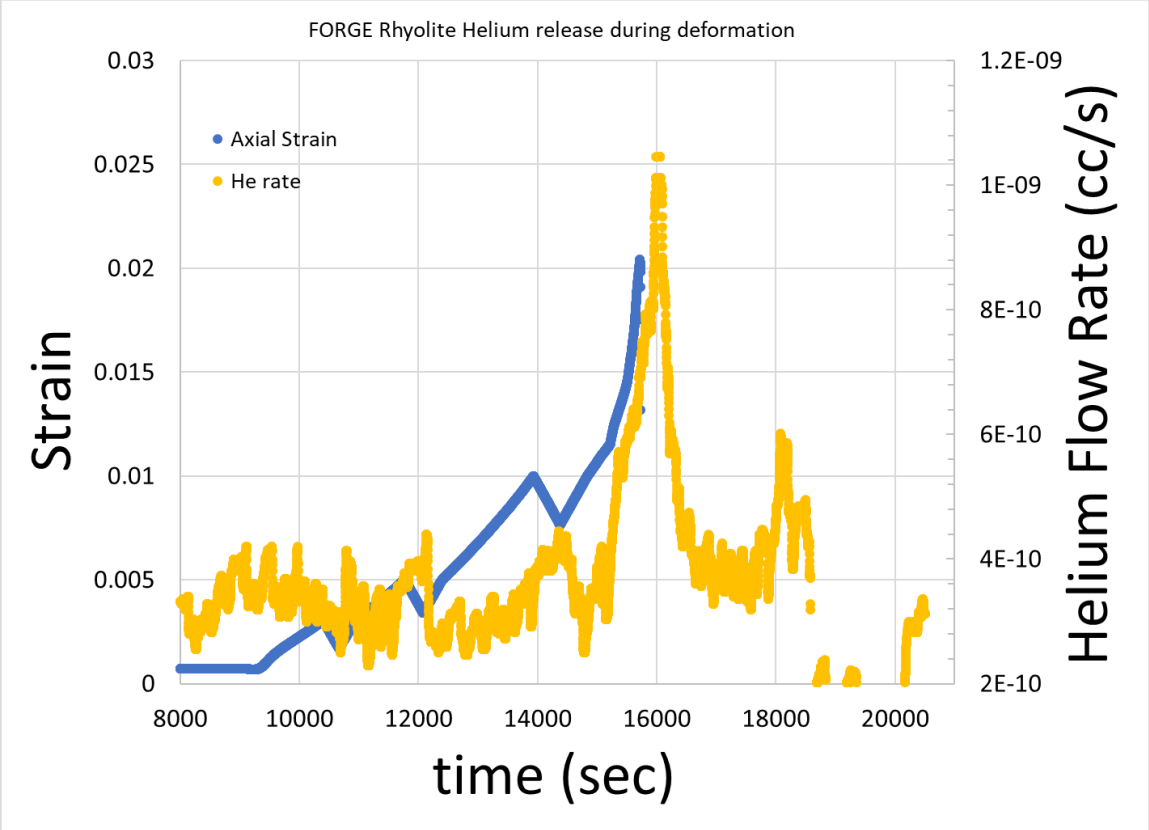

Figure 12. Strain and helium release versus time of rhyolite

Discussion and conclusions

In the above we have developed a data set for two analogue lithologies, deemed to be lithologic equivalents in the subsurface for the FORGE project. The mechanical properties, predominantly index properties, may be used in analyses to determine large scale rock response. Some properties determined appear to be relatable to density, which may make it easier to understand potential heterogeneity by simply measuring density. Elastic properties appear to be pressure dependent, this should be considered in future studies.

The flow through experiment shows that flow rate (permeability) decreases with increasing pressure, and increases during fracturing and during slip along those fractures, this is consistent with the “shear stimulation” concept. The helium release experiment contains the data to relate natural tracer (noble gases) release to deformation. The rhyolite studied likely contained only a small amount of noble gas, because of its fine grain size and near surface exposure and dramatic daily temperature swings during the past many millions of years. In the subsurface, there is opportunity to evaluate this technique with less weathered lithologies.

References

Stewart (1980), Geology of Nevada, Nevada Bureau of Mines and Geology Spec. Pub. 4.

Bauer, S. J., W. P. Gardner, and H. Lee (2016), Release of radiogenic noble gases as a new signal of rock deformation, Geophys. Res. Lett., 43, 10,688–10,694, doi:10.1002/2016GL070876.

Bauer, S. J., W. P. Gardner, and H. Lee (2017), Noble Gas Release and Flow Through a Granite and Basalt, PROCEEDINGS, 42nd Workshop on Geothermal Reservoir Engineering Stanford University, Stanford, California, February 13-15, 2017 SGP-TR-212

Lee M.Y. and Bauer, S.J.: (2015) Development of Helium-Mass-Spectrometry-Permeameter for the Measurement of Permeability of Near-Impermeable Rock. Rock Mechanics and Rock Engineering, DOI: 10.1007/s00603-016-1058-1